LA-4932

C. 3

Two-Dimensional, Continuous, Multicomponent Eulerian Calculations of Interactions of Shocks with V Notches, Voids, and Rods in Water

los alamos
scientific laboratory
of the University of California
LOS ALAMOS, NEW MEXICO 87544

UNITED STATES
ATOMIC ENERGY COMMISSION
CONTRACT W-7405-ENG. 36

Printed in the United States of America. Available from
National Technical Information Service
U. S. Department of Commerce
5285 Port Royal Road
Springfield, Virginia 22151
Price: Printed Copy $3.00; Microfiche $0.95

LA-4932
UC-34
ISSUED: May 1972

los alamos
scientific laboratory
of the University of California
LOS ALAMOS, NEW MEXICO 87544

Two-Dimensional, Continuous, Multicomponent Eulerian Calculations of Interactions of Shocks with V Notches, Voids, and Rods in Water

by

Charles L. Mader
James D. Kershner

TWO-DIMENSIONAL, CONTINUOUS, MULTICOMPONENT EULERIAN CALCULATIONS OF INTERACTIONS OF SHOCKS WITH V NOTCHES, VOIDS, AND RODS IN WATER

by

Charles L. Mader and James D. Kershner

ABSTRACT

The new two-dimensional, multicomponent, continuous Eulerian hydrodynamic code, 2DE, has been used to study the interaction of shocks with cylindrical aluminum rods, V notches, and cylindrical voids in water. Agreement between the computations and the previously reported photographic and PHERMEX radiographic study of the systems was within the resolution of the experimental data.

I. INTRODUCTION

The interaction of a shock wave with a cylindrical aluminum rod, a V notch, and a cylindrical void in water has been studied experimentally using the Los Alamos Scientific Laboratory "PHERMEX" radiographic facility and using framing cameras. The systems were further studied numerically using the PIC technique for solving the two-dimensional hydrodynamics. The results of the experimental and theoretical study were described in a report by Mader, Taylor, Venable and Travis.[1] They suggested that the experimental results could be used in evaluating numerical hydrodynamic techniques for treating such greatly distorted, complex, multicomponent flow problems.

The two-dimensional, multicomponent, continuous Eulerian hydrodynamic code, 2DE,[2] was designed to solve such flow problems, so we decided to follow our own good advice and test the new 2DE code by comparing the previously reported experimental results with 2DE calculations for the same systems. This report describes the results of that study.

II. COMPUTATIONAL METHOD

The 2DE code[2] computes two-dimensional, reactive, multicomponent hydrodynamic problems in slab or cylindrical geometry using continuous Eulerian equations of motion, realistic equation of state treatments for mixed cells, and the donor-acceptor-cell method to calculate multi-material cell fluxes.

The explosive-Plexiglas driving system was approximated, as in Ref. 1, as a constant-velocity piston whose velocity was adjusted to give the experimentally observed unperturbed position of the shock as it interacted with the density discontinuity. The equation of state parameters for water and aluminum were identical to those used in Ref. 1. The calculations were performed using 100 square cells in the Z direction and 50 in the R direction. The calculations required approximately 10 min. of 7600 computer time for each system studied. One Los Alamos atmosphere of air was used as the second component in the V-notch and cylindrical-void calculations. This eliminated the problems associated with attempting to program the interface movement that is characteristic of one-component continuous Eulerian treatments.

III. RESULTS

The experimentally observed interaction of a shock with an aluminum rod in water is well described by the computations, as is shown in Table I. Radiographs and sketches of the PHERMEX results are shown

TABLE I

EXPERIMENTAL RESULTS AND COMPUTATIONS
OF INTERACTION OF A SHOCK WITH A 1-CM-RADIUS ALUMINUM ROD IN WATER

	Time after Shock Arrived at Plexiglas-Water Interface							
	4.9 μsec		6.0 μsec		8.1 μsec		9.5 μsec	
	Exp.	Comp.	Exp.	Comp.	Exp.	Comp.	Exp.	Comp.
Axial thickness (height) of Al rod (cm)	1.89	1.90	1.67	1.70	1.70	1.60	1.60	1.50
Radial thickness (width) of Al rod (cm)	2.00	2.00	2.10	2.10	2.20	2.40	2.30	2.45
Axial distance of shock wave above top of Al rod (cm)	-	-	-	-	0.45	0.40	0.70	0.60
Radial distance of reflected shock wave along axis of Al rod (cm)	1.20	1.20	1.90	1.85	3.20	3.10	3.90	3.80

in Fig. 1, and the 2DE results are shown in Figs. 2-6.

The experimentally observed interaction of a shock with a V notch in water also appears to be well described by the computations, as is shown in Table II. Radiographs and sketches of the PHERMEX results are shown in Fig. 7, and the 2DE results are shown in Figs. 8-12. We plan to study the interaction of a shock with a V notch in aluminum using the 2DE code as soon as it has realistic descriptions of two-dimensional elastic-plastic flow and spalling. As described in Ref. 1, fluid computations that do not include spalling or elastic-plastic flow yield similar results for water and aluminum V notches. Although such computations reproduce the water V-notch radiographic results, they are completely inadequate to describe the aluminum V notch PHERMEX observations.

TABLE II

EXPERIMENTAL RESULTS AND COMPUTATIONS OF INTERACTION OF A SHOCK WITH A V NOTCH IN WATER

	Time After Shock Arrived at Plexiglas-Water Interface			
	2.5 μsec		3.5 μsec	
	Exp.	Comp.	Exp.	Comp.
Distance of jet peak above initial apex of V notch (cm)	0.90	0.85	1.45	1.50
Distance of lowest part of jet above initial apex of V notch (cm)	0.70	0.68	1.10	1.10

The experimental radiographs and the computations for the interaction of a shock with a cylindrical void in water agree well except near the time of void closure as is shown in Table III. Framing-camera pictures of the void closure suggest that interpretation of the PHERMEX radiographs is difficult because of large density gradients, as is discussed in Ref. 1. The computations and framing-camera pictures agree within the resolution of the experimental results. Radiographs of the PHERMEX results are shown in Fig. 13, and framing-camera pictures are shown in Fig. 14. The 2DE results are shown in Figs. 15-19.

The contour intervals for Figs. 2-6 and 15-19 are 0.1 g /cm^3, 0.01 mbar, 200°K, and 0.01 cm/μsec. The contour intervals for Figs. 8-12 are 0.2 g /cm^3, 0.02 mbar, 100°K, 0.01 cm/μsec for velocity in the R direction, and 0.02 cm/μsec for velocity in the Z direction. The locations of the mixed cells are shown by asterisks.

TABLE III

EXPERIMENTAL RESULTS AND COMPUTATIONS OF INTERACTION OF A SHOCK WITH A CYLINDRICAL VOID IN WATER

	Time After Shock Arrived at Plexiglas-Water Interface					
	4.9 μsec		5.9 μsec		7.6 μsec	
	Exp.	Comp.	Exp.	Comp.	Exp.	Comp.
Axial distance of jet above initial bottom of void (cm)	0.70	0.60	1.30	1.20	2.40	2.50

IV. CONCLUSIONS

Agreement between the dynamic radiographs and the numerical 2DE computations of the interaction of a shock with an aluminum rod, a V notch in water, and a cylindrical void in water is within the experimental resolution of approximately ± 5%.

REFERENCES

1. Charles L. Mader, Roger W. Taylor, Douglas Venable, and James R. Travis, "Theoretical and Experimental Two-Dimensional Interactions of Shocks with Density Discontinuities," Los Alamos Scientific Laboratory report LA-3614 (1967).

2. James D. Kershner and Charles L. Mader, "2DE: A Two-Dimensional Continuous Eulerian Hydrodynamic Code for Computing Multicomponent Reactive Hydrodynamic Problems," Los Alamos Scientific Laboratory report LA-4846 (1972).

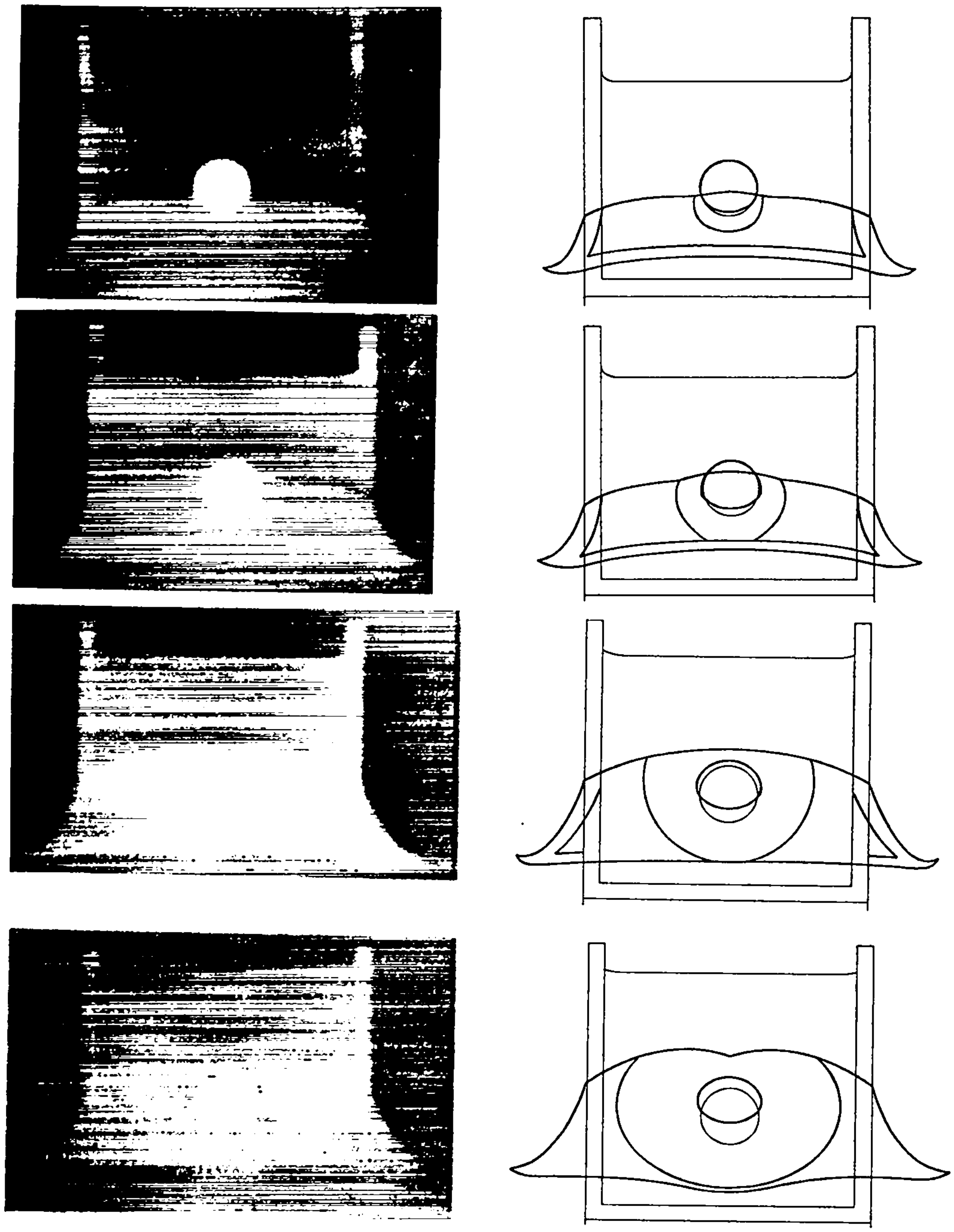

Fig. 1. Radiographs and sketches of prominent features of the interaction of a shock in water with a 1-cm-radius aluminum rod at 4.9, 6.0, 8.1, and 9.5 μsec after the shock wave arrived at the water-Plexiglas interface.

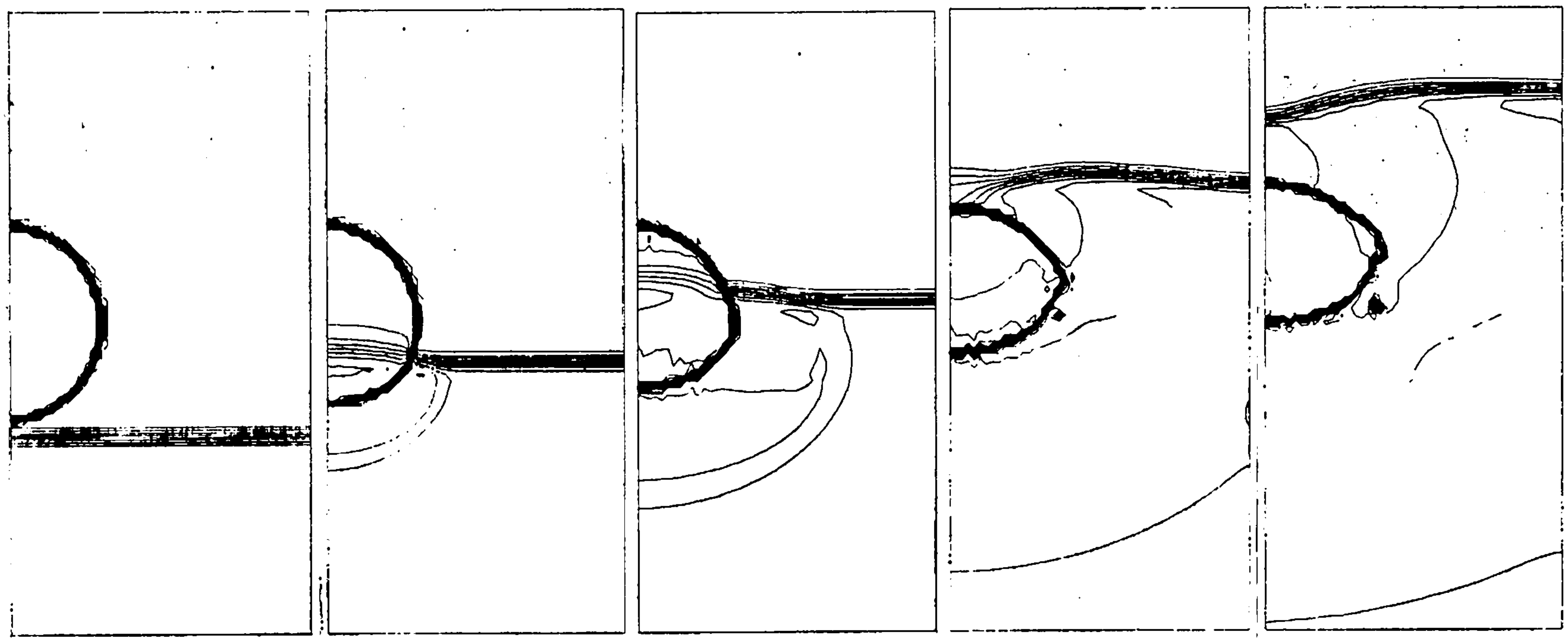

Fig. 2. The isopycnics for the computed interaction of a shock in water with a 1-cm-radius aluminum rod at 3.6, 4.9, 6.0, 8.0, and 9.5 μsec. A constant-pressure, 155-kbar piston is assumed, and the rod is centered 3.25 cm above it.

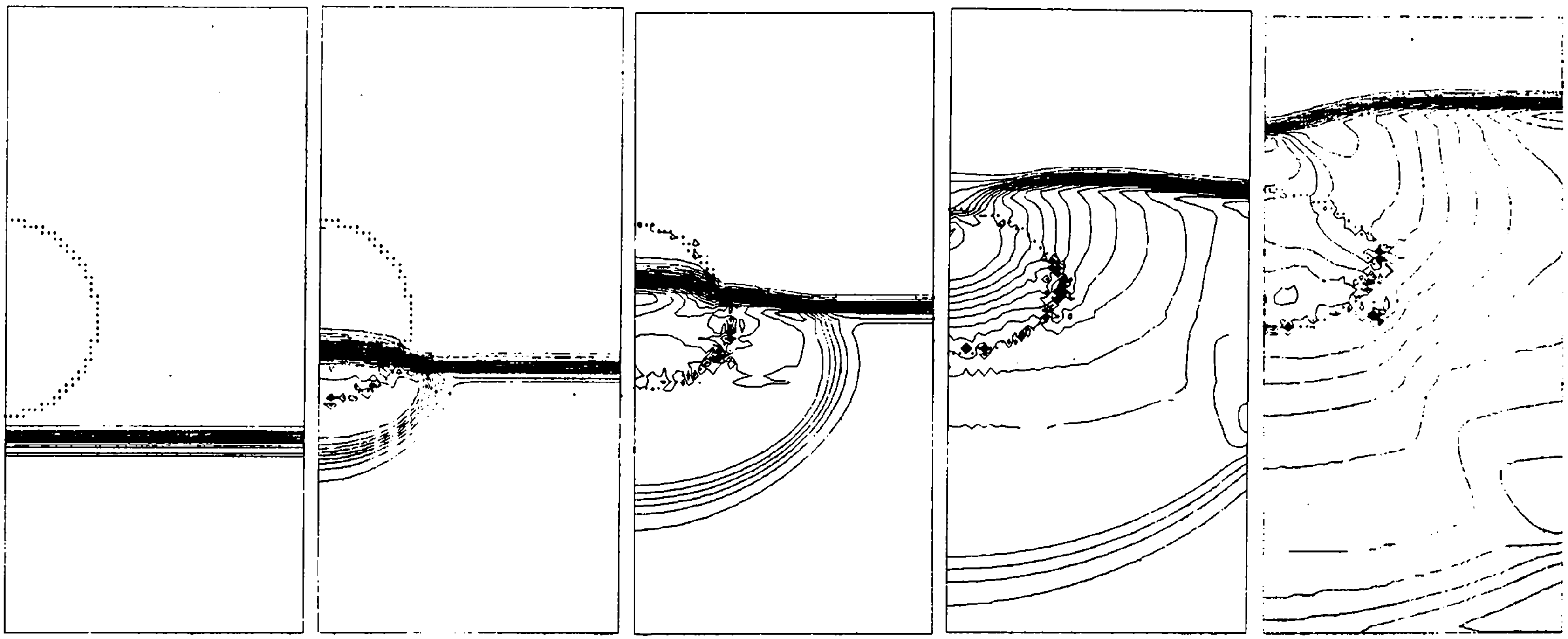

Fig. 3. The isobars for the computed interaction shown in Fig. 2.

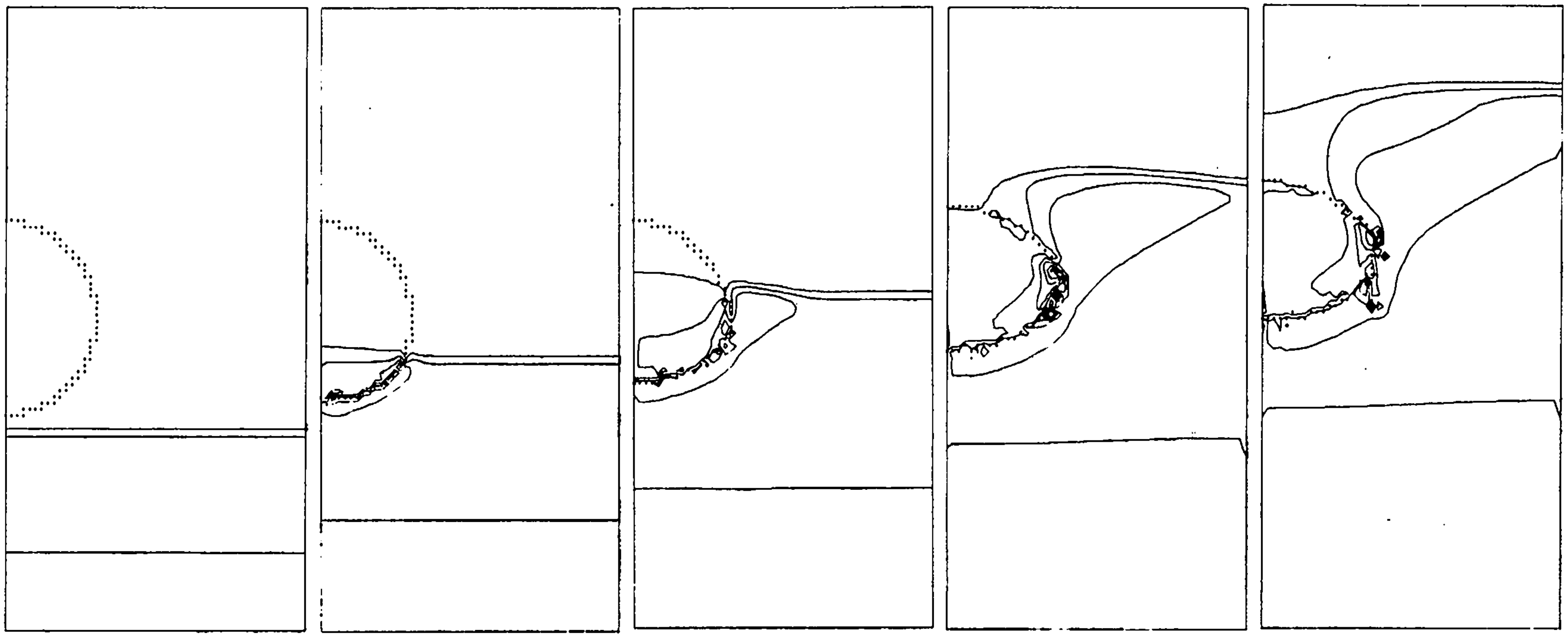

Fig. 4. The isothermal plots for the computed interaction shown in Fig. 2.

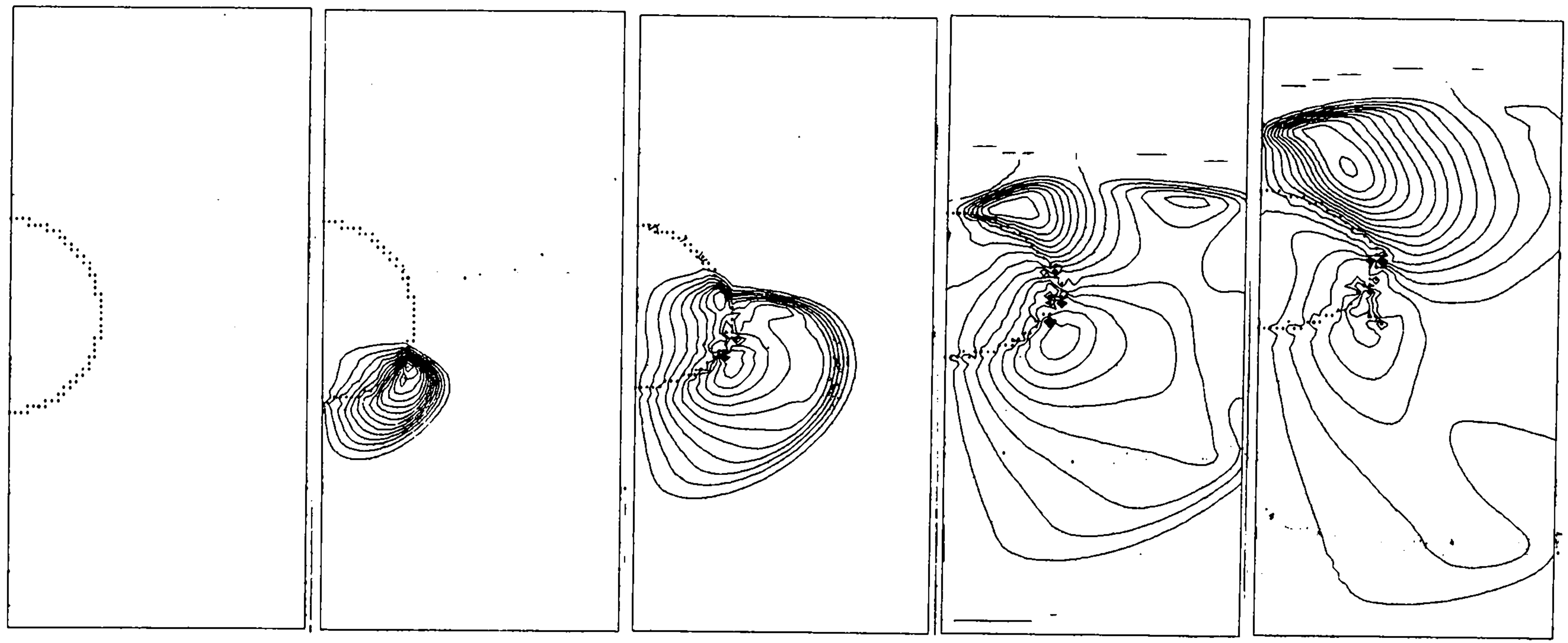

Fig. 5. The R-direction isovelocity plots for the computed interaction shown in Fig. 2.

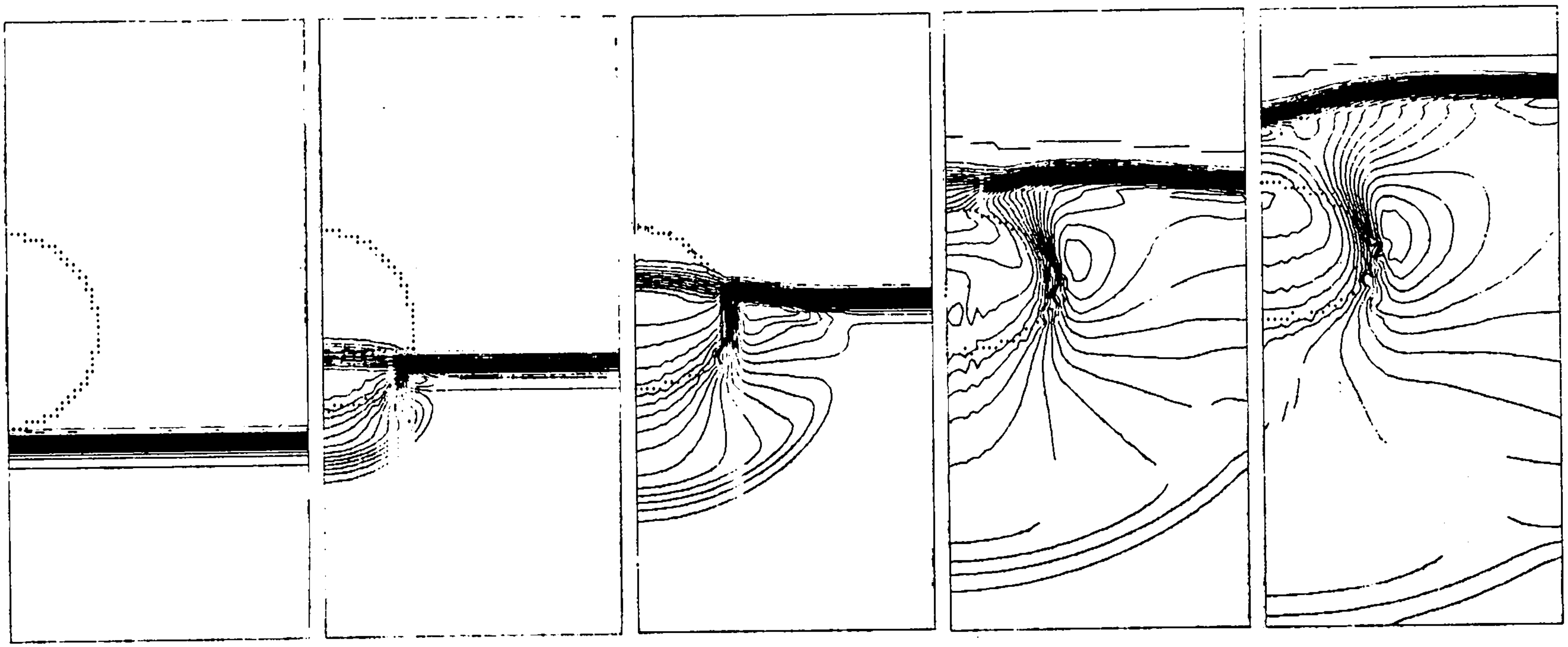

Fig. 6. The Z-direction isovelocity plots for the computed interaction shown in Fig. 2.

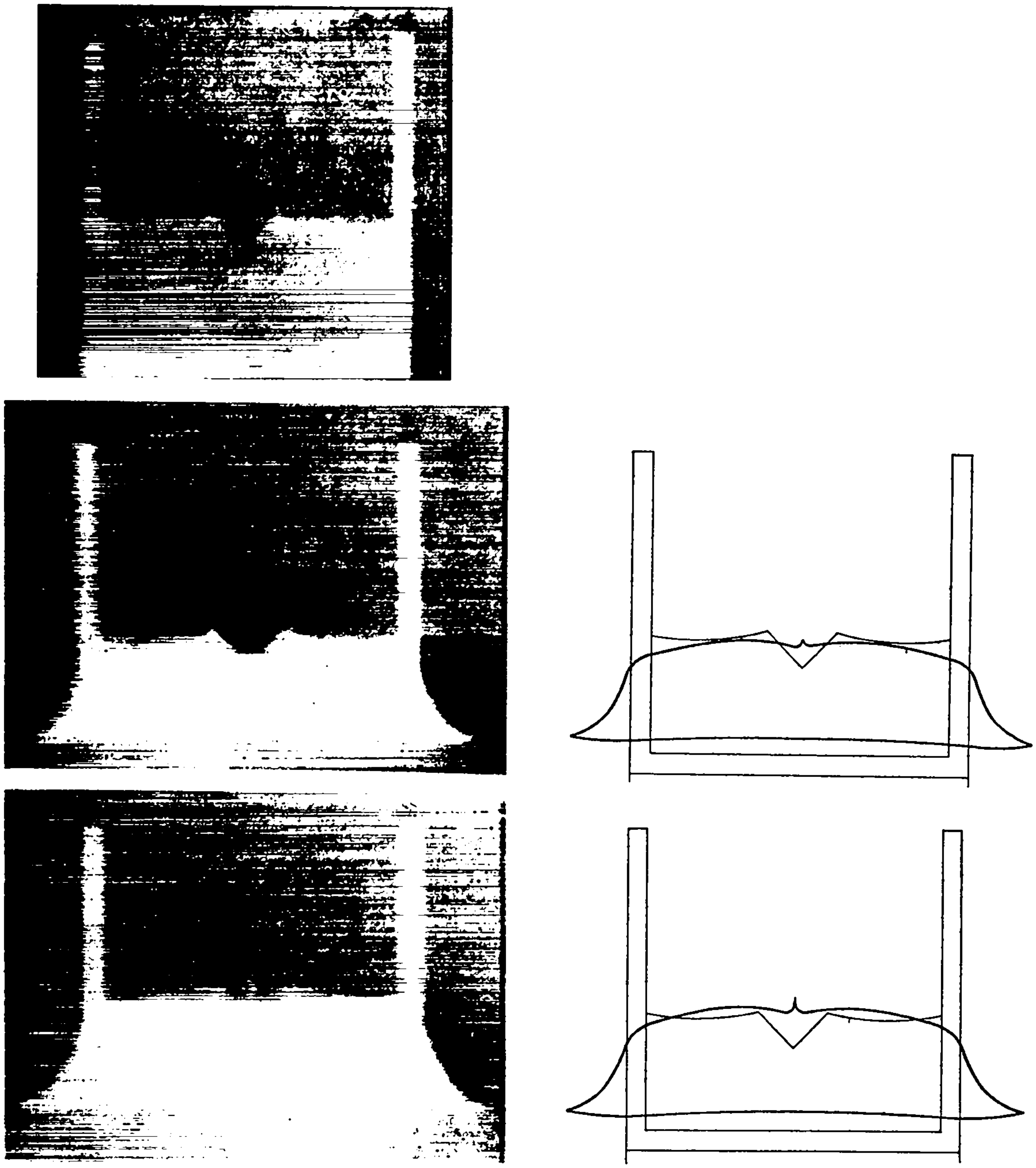

Fig. 7. Radiographs and sketches of prominent features of the interaction of a shock in water with a 1-cm-deep V notch at 0.0, 2.5, and 3.5 μsec. The apex of the notch is 0.5 cm above the piston.

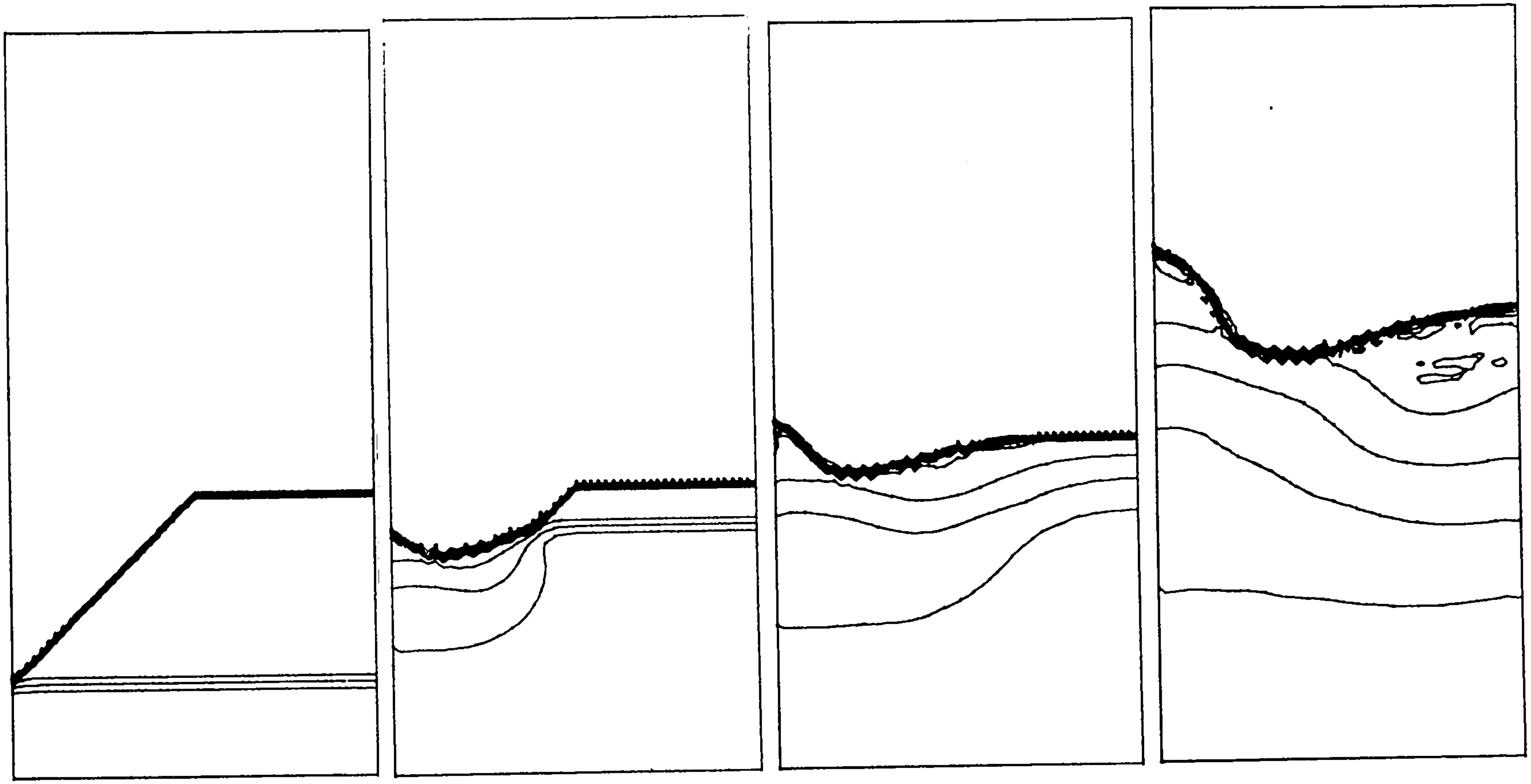

Fig. 8. The isopycnics for the computed interaction of a shock in water with a 1-cm-deep V notch at 1.0, 2.5, 3.5, and 5.0 μsec. A constant-pressure, 121-kbar piston is assumed, and the apex of the notch is 0.5 cm above it.

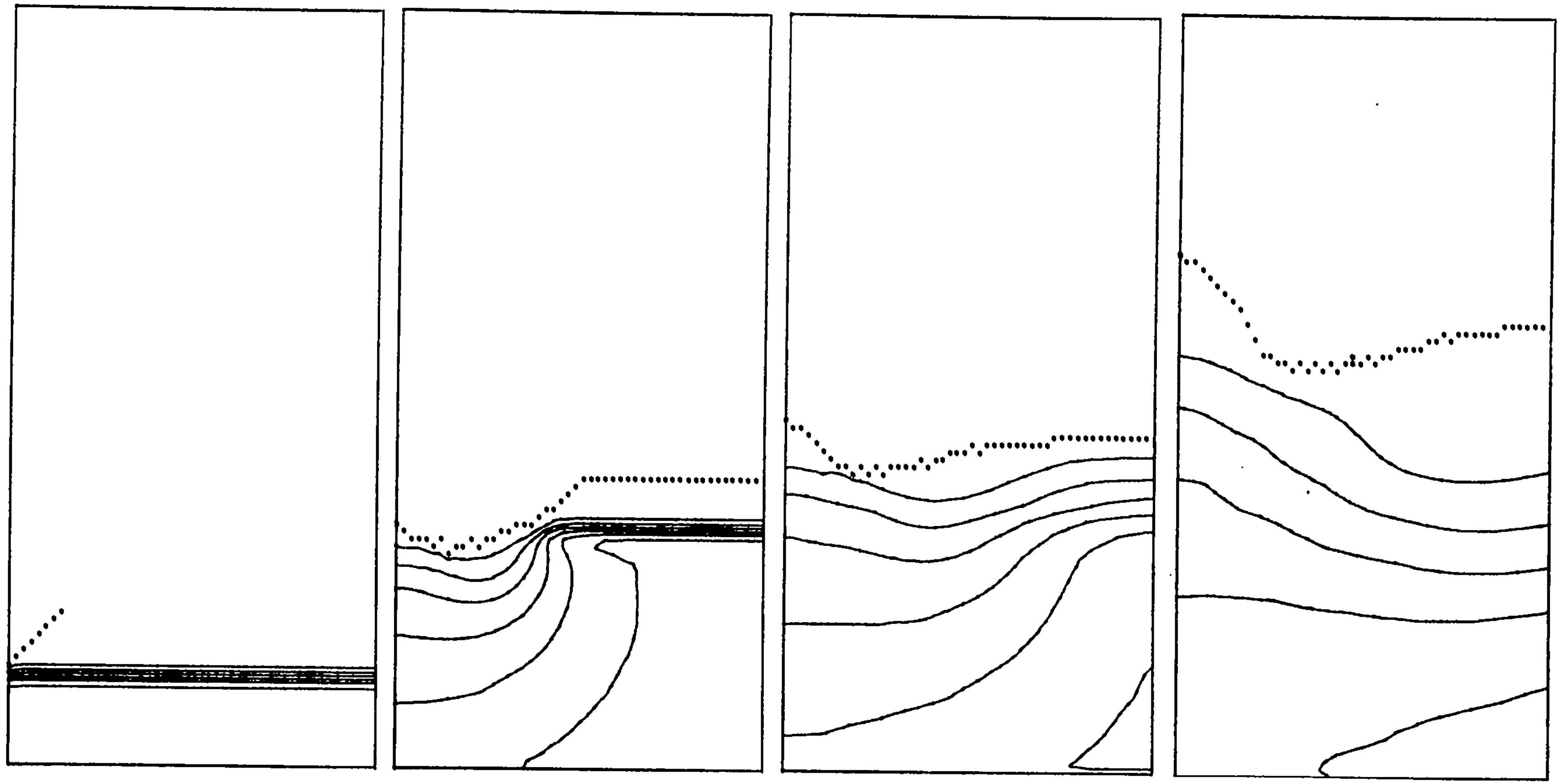

Fig. 9. The isobars for the computed interaction shown in Fig. 8.

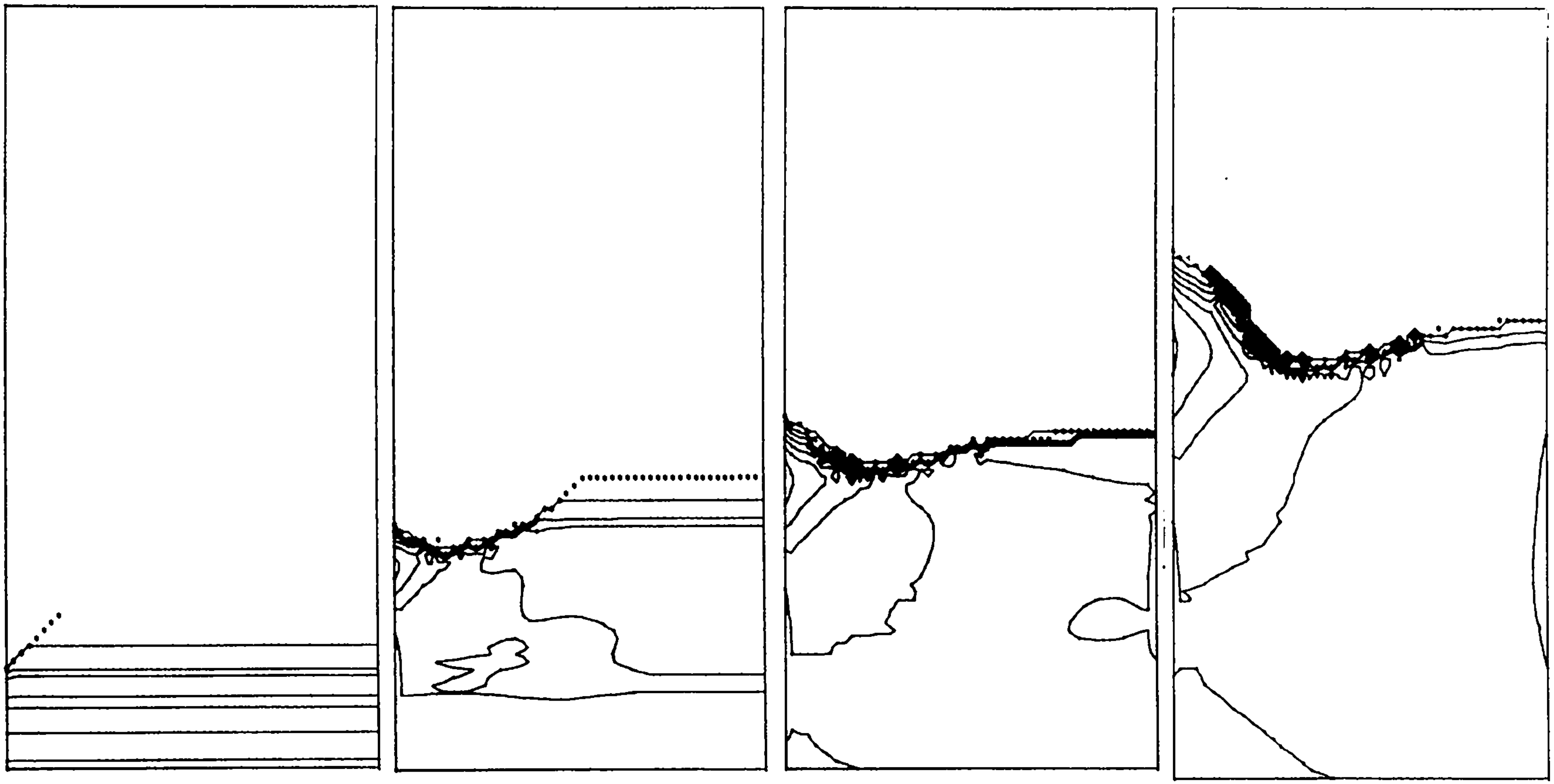

Fig. 10. The isothermal plots for the computed interaction shown in Fig. 8.

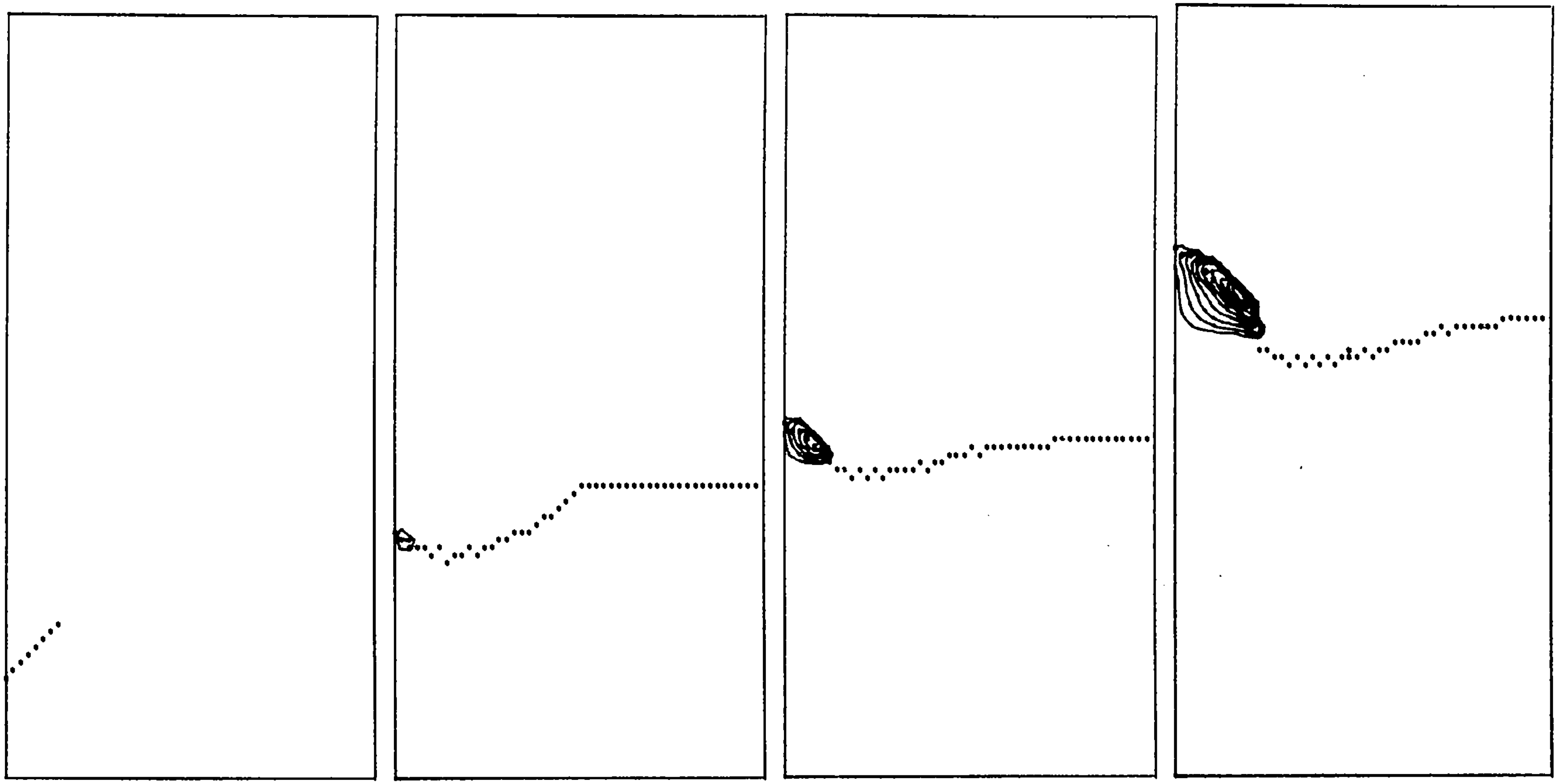

Fig. 11. The R-direction isovelocity plots for the computed interaction shown in Fig. 8.

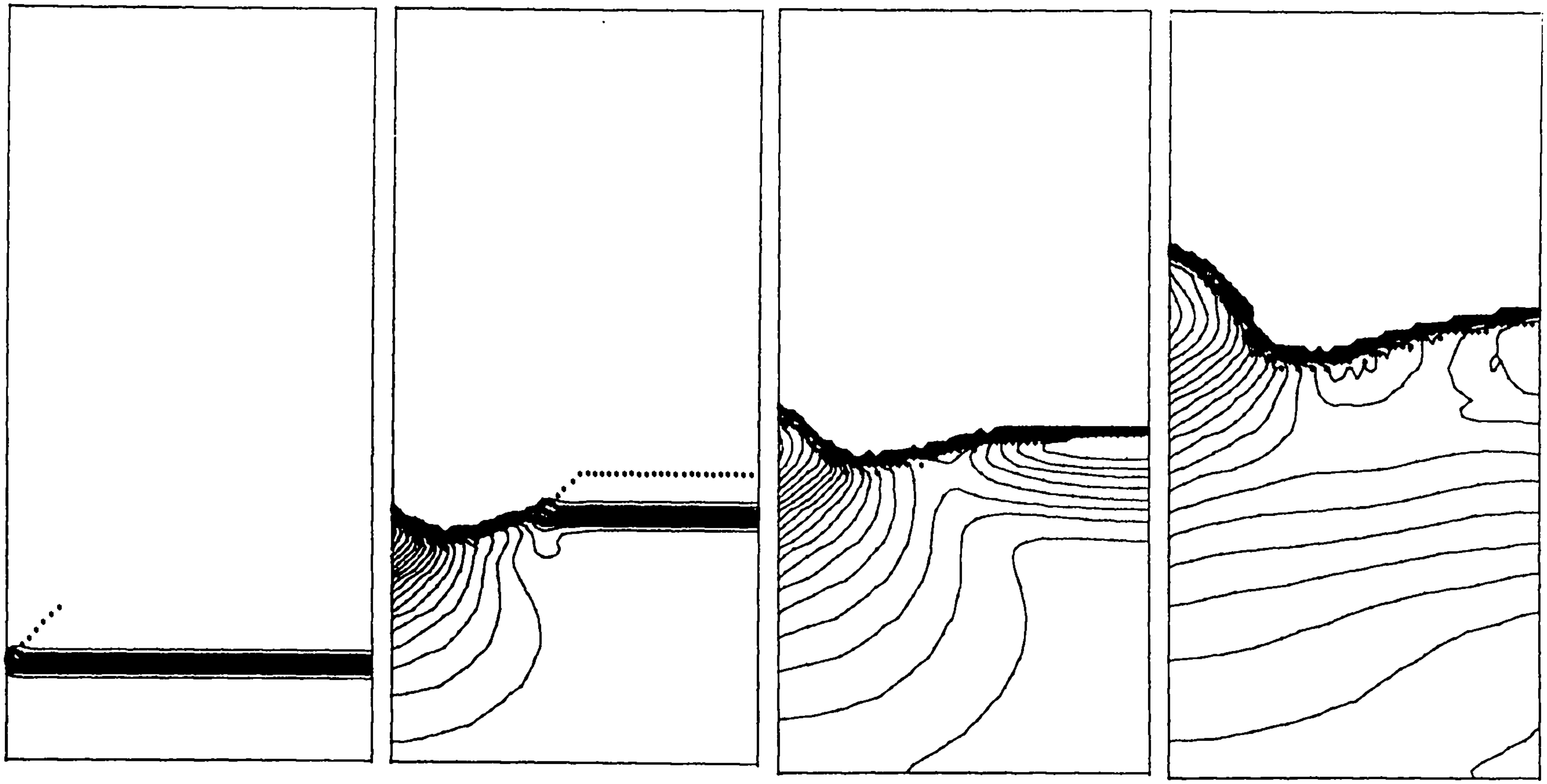

Fig. 12. The Z-direction isovelocity plots for the computed interaction shown in Fig. 8.

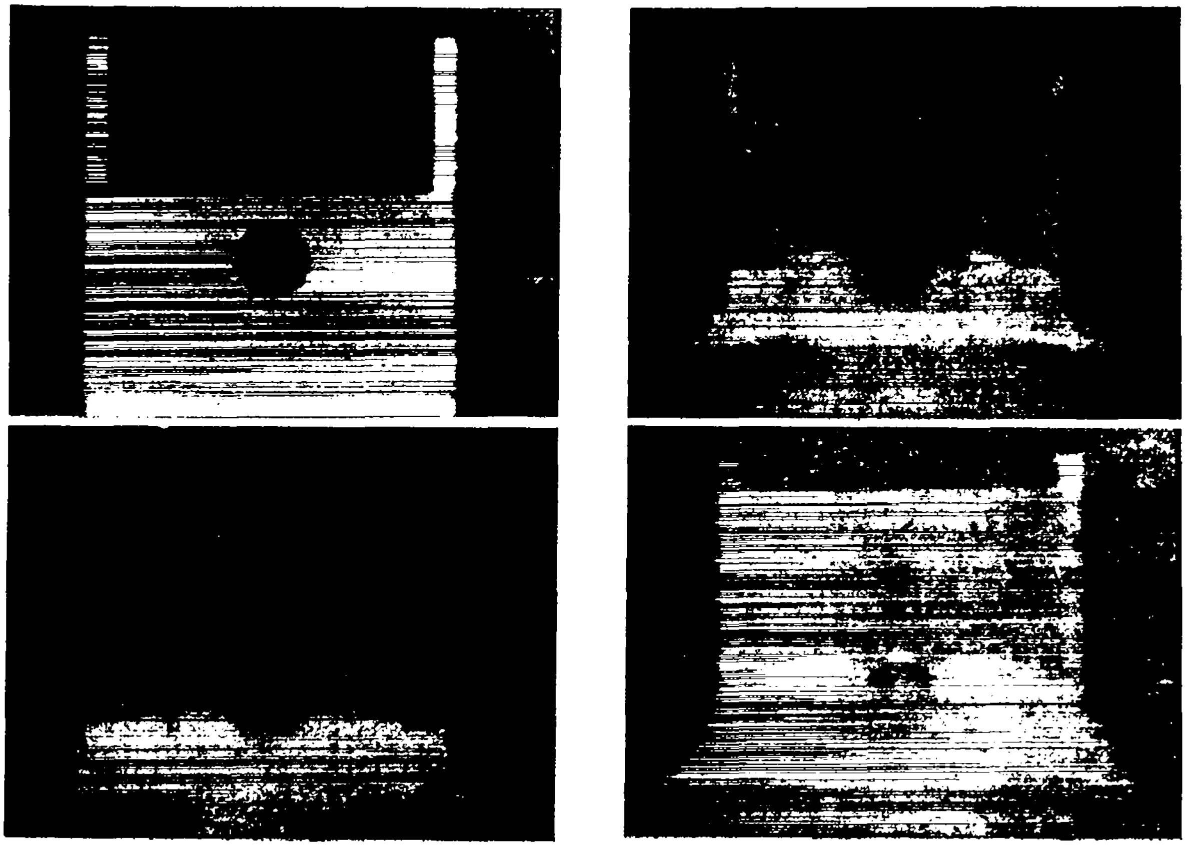

Fig. 13. PHERMEX radiographs of a 1-cm-radius cylindrical void in water centered 3.25 cm above the inside bottom of a Plexiglas box at 0.0, 4.9, 5.9, and 7.6 μsec after the shock arrived at the Plexiglas-water interface. The cylindrical void was formed by a thin-walled (0.006-in.) glass tube.

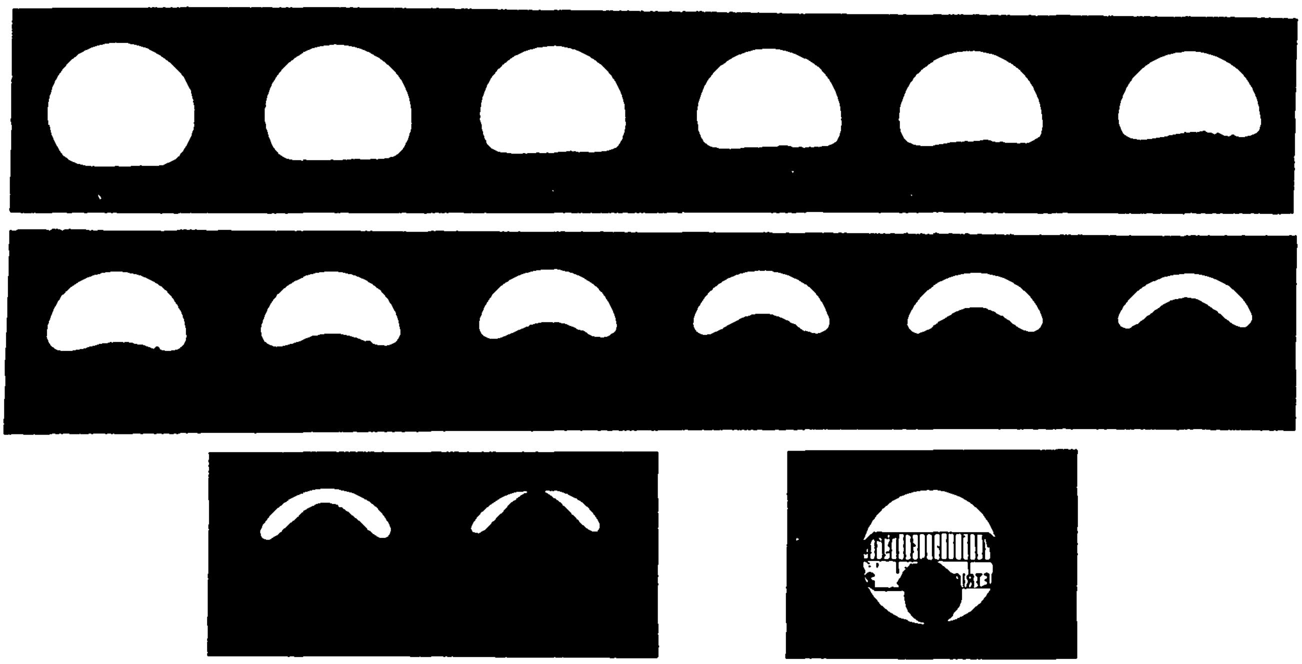

Fig. 14. Framing-camera photographs of the closure of a 1-cm-radius cylindrical void in polyethylene in the same geometry as that in Fig. 13. Time between frames is 0.21 μsec, and exposure time is 0.09 μsec. The last frame is a still photograph.

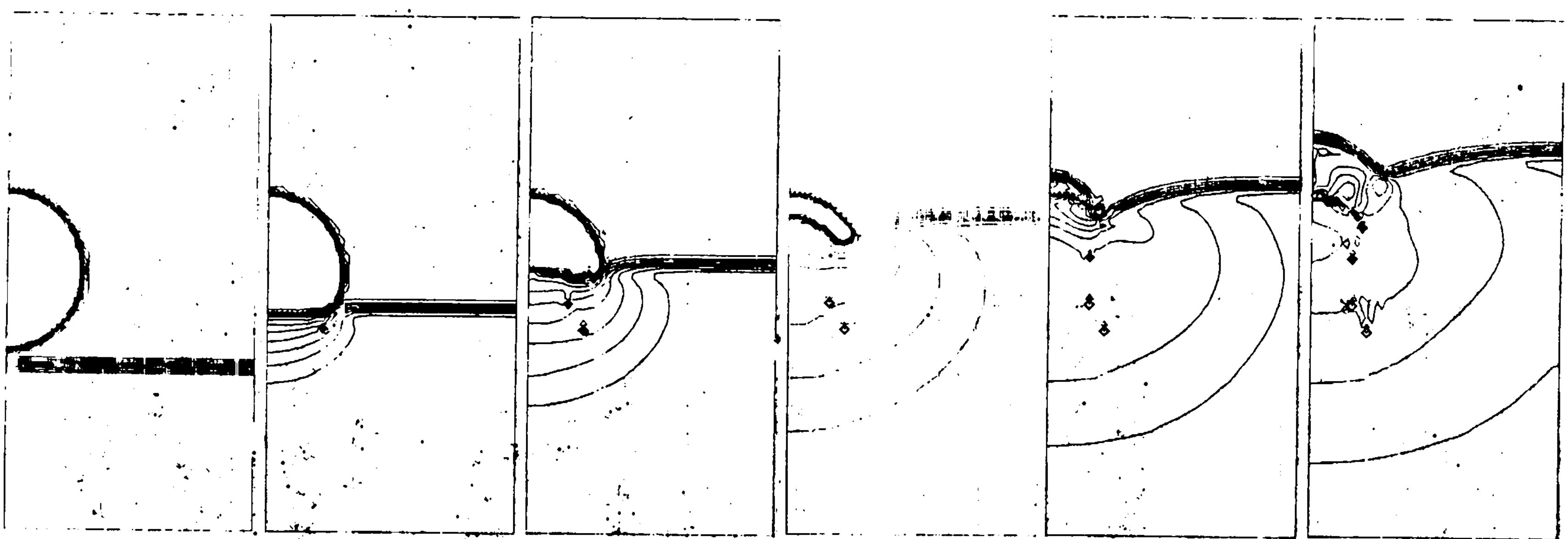

Fig. 15. The isopycnics for the computed interaction of a shock with a 1-cm-radius cylindrical hole containing one Los Alamos atmosphere of air and centered 3.25 cm above a constant-pressure, 155-kbar piston. Times are 3.6, 4.9, 5.9, 6.9, 7.6, and 8.4 μsec.

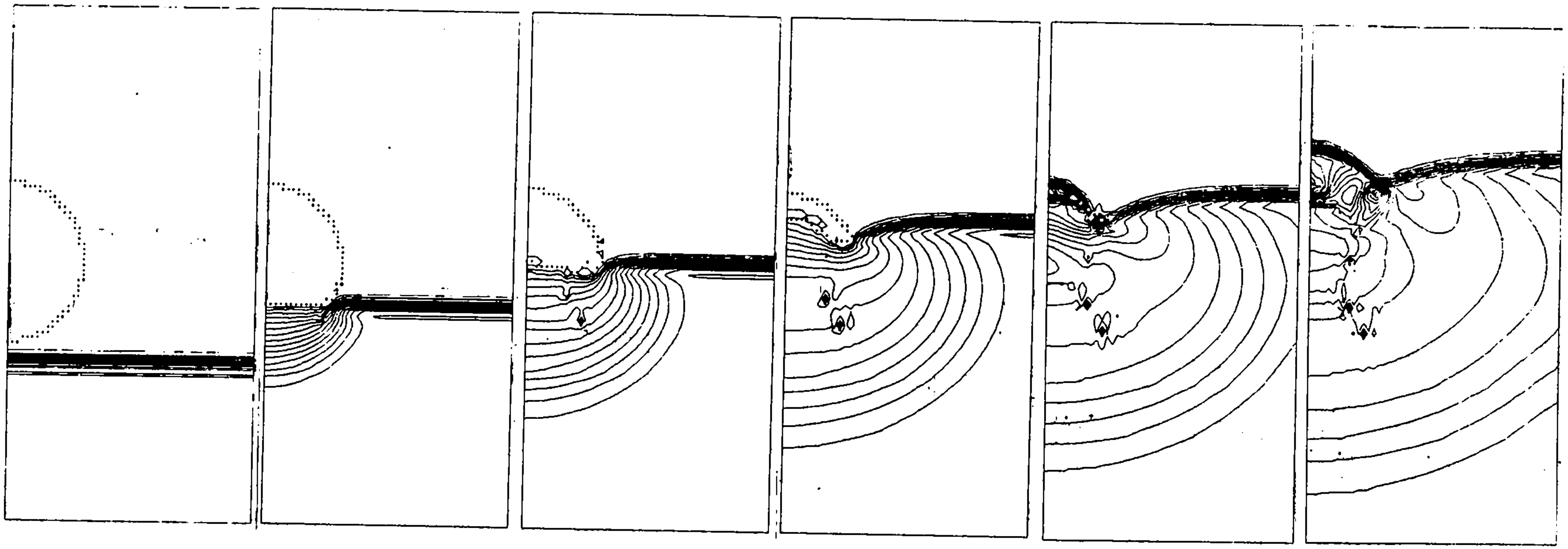

Fig. 16. The isobars for the computed interaction shown in Fig. 15.

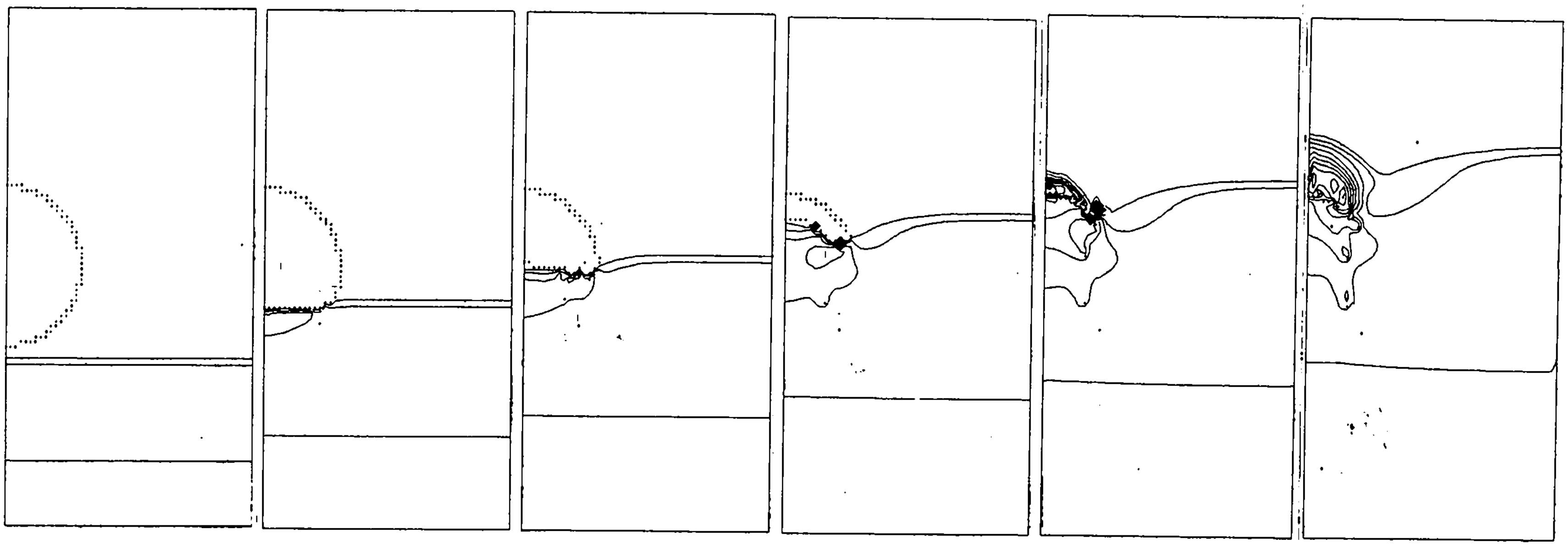

Fig. 17. The isothermal plots for the computed interaction shown in Fig. 15.

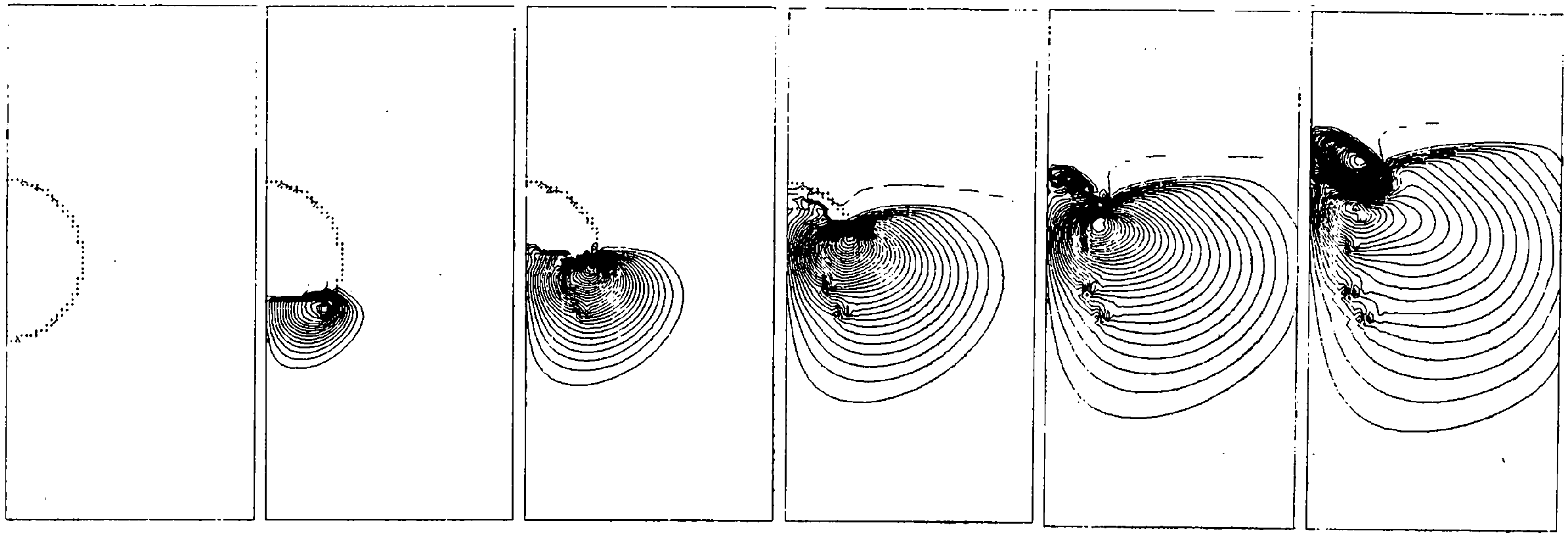

Fig. 18. The R-Direction isovelocity plots for the computed interaction shown in Fig. 15.

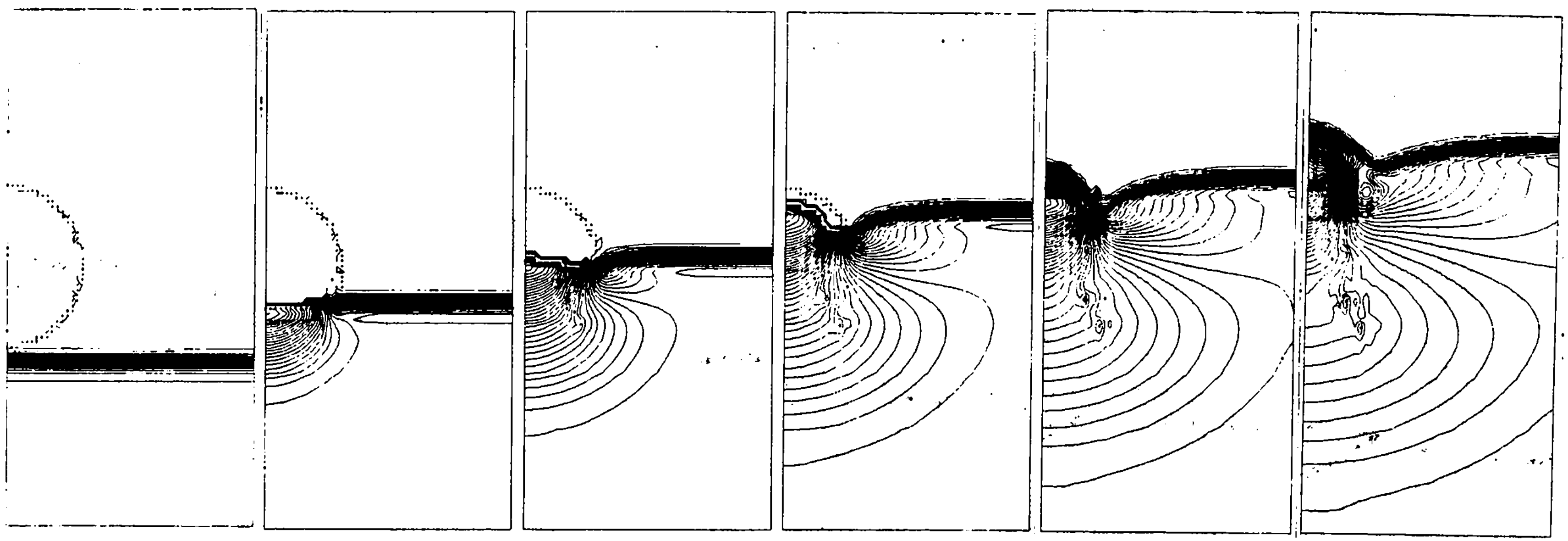

Fig. 19. The Z-direction isovelocity plots for the computed interaction shown in Fig. 15.